DOI: https://doi.org/10.54966/jreen.v28i1.1344

Journal of Renewable Energies

Revue des Energies Renouvelables

journal home page: https://revue.cder.dz/index.php/rer

Conference paper

Impact of using corrugated wall and nanofluid on the performance improvement of thermoelectric generator mounted channels

Hessem Djeddou [a,*], **Brahim Fersadou** [a], **Henda Kahalerras** [a], **Mohamed Benelhaoues** [a]

[a] *Laboratory of Multiphase Flows and Porous Media, University of Sciences and Technology Houari Boumedienne, FGMGP, BP 32 El Alia 16111 Bab Ezzouar, Algiers, Algeria*

ARTICLE INFO

Article history:

Received January 12, 2025

Accepted January 29, 2025

Keywords:

Heat transfer,
Thermoelectric generator,
Nanofluid,
Wavy wall,
Fluid flow.

ABSTRACT

The influence of using a corrugated wall as a passive heat transfer enhancement technique for the sake of improving the power generation of thermoelectric generator (TEG) located in between two corrugated channels flowing nanofluid has been numerically examined. The upper and the lower channels carry hot and cold water-based single-walled carbon nanotube nanofluid (SWCNT), respectively. Finite element method, FEM, is chosen to tackle the 3D steady-state equations governing the TEG with associated boundary conditions. Several parameters related to the performance of thermoelectric generator such as Reynolds number (between 50 and 1000) and the number of corrugations (between 1 and 5) were in depth assessed. The findings indicate that the Reynolds number plays a significant role in improving thermoelectric power generation. When the Reynolds number increases, TEG produces a higher electric power value. However, the results also reveal that the number of corrugations has a limited impact on the performance of TEG.

1. INTRODUCTION

As the world population is growing rapidly and the expansion of industrial activities is noticeably uncontrolled, the energy demand is continuously rising. Natural energy resources such as fossil fuels (oil, gas and coal) have been mainly the most available energy option used for centuries to eliminate the human energy needs. However, the extraction and exploitation of fossil fuels adversely contribute to many environmental issues and have been a matter of concern for decision-makers in addition to the depletion of natural energy resources at a high rate, The unavoidable effect of those natural resources on the environment, including climate change that poses a continuing threat on the planet, pollution and habitats destruction, and the nonrenewable nature of those resources raise the alarm, and finding alternatives has become one of the main responsibilities of the scientific community. From many

* *Corresponding author, E-mail address: djeddou.sam@gmail.com*

ISSN: 1112-2242 / EISSN: 2716-8247

available renewable energy technologies such as solar, wind, geothermal, thermoelectric energy technology is one of promising solutions for tackling those concerns for energy security at very low risk. Unfortunately, the applicability of those sustainable technologies in a wide range of domains is still facing challenges in terms of efficiency, cost and effectiveness. For that reason, developing and optimizing renewable energy technologies have been the center of interest for energy harvesting researchers. One of the renewable energy technologies that has received attention in recent years due to its advantages in producing free-carbon, environmentally friendly, low cost, low maintenance is thermoelectric generator.

Through a complex thermodynamic process, the function key of thermoelectric generator, TEG, is a straightforward alteration of heat energy into electric energy. This device, which consists of N-type and P-type pairs of dissimilar semiconductor materials, joined by electrodes (usually copper), interposed between two plates of ceramic acting as support of TEG and electric insulation (Zoui et al., 2020), and sandwiched between two distinctive heat exchangers (Luo et al., 2021).To produce maximum electricity, The P-type and N-type of TEG are assembled electrically in series and thermally in parallel. The working principle behind TEG is the Seebeck effect, discovered by Seebeck in 1821 (Polozine et al., 2014), converting must-available gradient temperature between the opposite sides of TEG into electrical energy by the thermo-physical characteristics of material employed. In light of its very low efficiency, between 5% and 10% (Scherrer et al., 2018), a considerable number of research studies have been carried out in order to improve thermoelectric conversion of the device. Many factors that affect TEG power production such as leg geometries, P type and N type pairs arrangements, material used and temperature gradient between TEG surfaces, have been investigated, but little is still conducted about enhancing heat transfer of TEG boundaries.

Thermoelectric generator has been widely used in many different fields including aerospace applications (LaLonde et al., 2011), energy source for wearable devices (Kim et al., 2018), recovering waste heat from the automotive industry (Mostafavi & Mahmoudi, 2018; Orr et al., 2017), recovering heat from industrial applications (Casi et al., 2021; Chen et al., 2022; Zhao et al., 2017) and medical applications as powering devices for physiology sensors (Proto et al., 2018; Wang et al., 2009).

There are many different materials used in manufacturing TEG module. The choice of material strongly depends on the temperature surrounding TEG device and the figure of merits z, which is a dimensionless value describing the conversion efficiency of TEG material. For example, bismuth telluride (Bi2Te3) is the most commonly used material when a low range of temperature is available, Lead (Pb) is preferable when temperature ranges between 450k and 850k, and silicon germanium(SiGe) is used at higher temperature (850 k<T<1300 K) (Aridi et al., 2021).

Numerous studies have been conducted numerically and experimentally to enhance thermoelectric conversion efficiency. Selimefendigil et al. (2023) conducted a numerical investigation of thermoelectric generator mounted triangular wavy channel with different shaped nanoparticles. The results show a significant increase in power generation when varying the amplitude of waves compared to the number of waves. In comparison with spherical shape, the cylindrical shape of nanoparticles has a noteworthy impact on producing power, and augmenting the volume fraction of nanoparticles produces higher energy. Nugraha et al. (2024) investigates numerically and experimentally the thermal characteristics of thermoelectric generator at different heat rates. It was found that the generated power of thermoelectric generator is higher when heating rate is slow. Selimefendigil and Öztop (2023) studied the impact of using helical coil on the performance enhancement of thermoelectric generator placed between channels. It was concluded that TEG produces more power when helical coils are installed in both channels, and the higher the number of turns the coil has, the more electric power is generated.

In this current work, enhancing thermoelectric energy conversion is the main objective of the study, and this can be accomplished by improving heat transfer rate between nanofluid and thermoelectric module, by using water-based single-walled carbon nanotubes (SWCNT) nanofluid and wavy (corrugated) channel as a passive technique for augmenting heat transfer.

2. NUMERICAL METHODS

2.1 TEG Mounted Wavy Channel

Figure (1) presents a 2D and 3D schematic view of thermoelectric generator (TEG) mounted two wavy channels employed in the study, composing of P and N-type of semiconductors. The hot nanofluid runs into the upper channel whereas the cold nanofluid flows in the lower channel. The following formulas describe the profile of both upper and lower wavy channels, respectively.

$$f(x) = 1 - Amp[1 - cos(n\pi x)] \quad (1)$$

$$f(x) = Amp[1 - \cos(n\pi x)] \quad (2)$$

Amp denotes the amplitude of the wave, and n represents the number of waves.

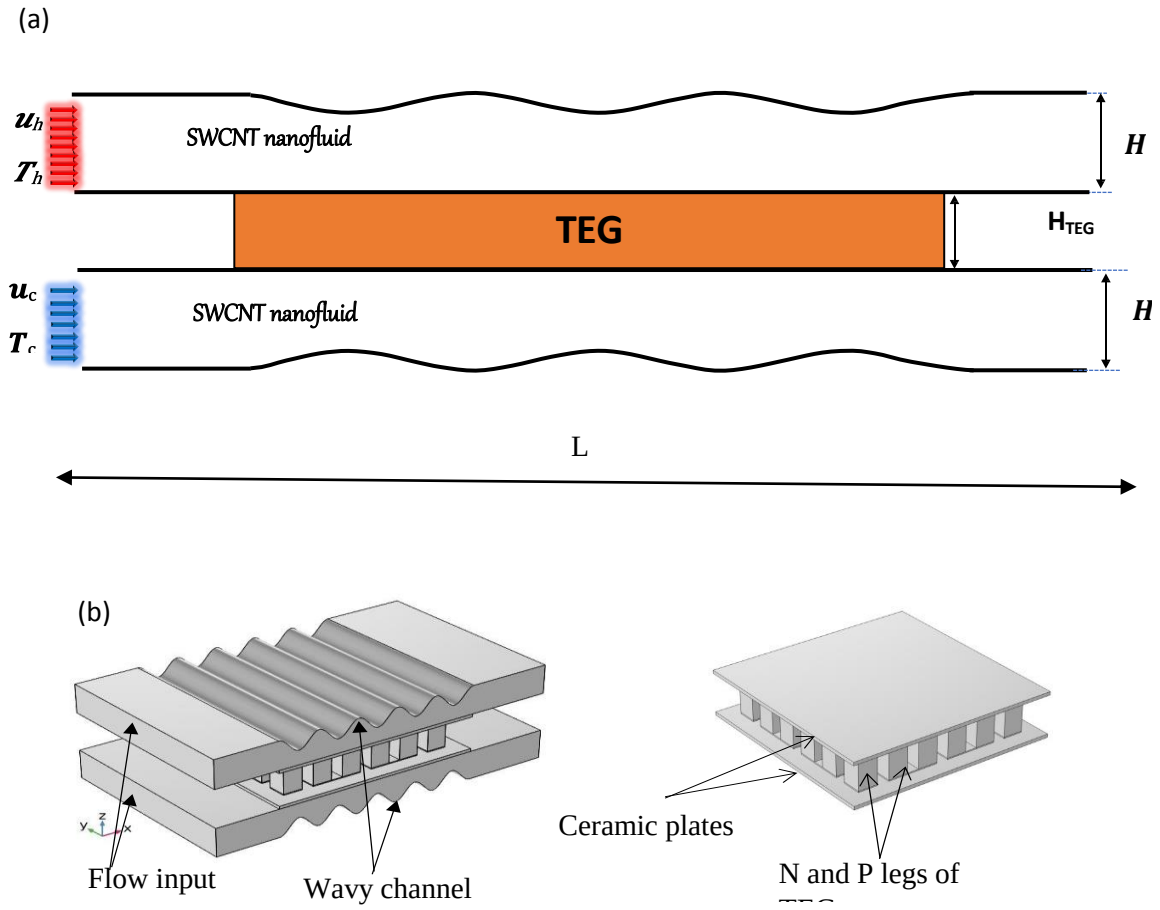

Fig 1. 2D (a) and 3D (b) schematic view of thermoelectric generator mounted channels

The length (L), width (W) and height (H) of both channels are 21mm,16mm and 3mm, respectively. The TEG module under study is made up of 32 legs of P-type and N-type of bismuth telluride (Bi_2Te_3)

material, copper as conductor, joining P and N legs, and two ceramic plates as electric insulators. The geometry of legs is 1.5mm for the length, 1.5mm for the width and 3.2mm for the height. copper length, width and height are 3.9mm,1.5mm and 0.1mm, respectively, and the thickness of ceramic plate is 0.3mm. the material properties of all the components of TEG module are shown in Table 1. Thermoelectric module, which works under the Seebeck effect, transforms heat energy into electrical energy through the physical properties of semiconductors. The mechanism of harvesting electrical energy is achieved through the presence of temperature gradient between the upper and lower surfaces of ceramic plates of TEG.

Table1. Material properties of TEG

	Symbol	P-type leg (Bi_2Te_3)	P-type leg (Bi_2Te_3)	Electrode (Copper)	Ceramic (Alumina)
Thermal conductivity	k (W/m K)	1.6	1.6	400	27
Electric conductivity	σ (S/m)	$0.8x10^5$	$0.81x10^5$	$5.9x10^8$	-
Seebeck coefficient	s (V/K)	$2.1x10^{-4}$	$-2.1x10^{-4}$	$6.5x10^{-6}$	-
Heat capacity	c_p(J/kg K)	154	154	385	900
Density	ρ (kg/m^3)	7700	7700	8960	3900

This study was conducted under the following assumptions:

1. The flow of both channels is three dimensional, laminar, steady and incompressible
2. The study does not include Natural convection, Thermal radiation, and viscous dissipation
3. No internal heat generation
4. Temperature independence of the properties of nanofluids

The output voltage produced (v_{out}) from thermoelectric conversion where the temperature difference ($\Delta T = T_{hot} - T_{cold}$,) applied at the extremities of TEG is given as:

$$v_{out} = N s_{PN} \Delta T \tag{3}$$

Where N represents the number of pairs the TEG has, and s_{PN} expresses the Seebeck coefficient of P and N materials of TEG ($s_{PN} = s_P - s_N$). Thermoelectric generator material ought to have low thermal conductivity, high Seebeck effect and factor of merit (ZT) to obtain higher efficiency. ZT, which denotes the factor of merit, is expressed as:

$$ZT = (s^2 \sigma / k)\, T \tag{4}$$

The internal resistance of thermoelectric module is given as:

$$R_i = \left(R_p + R_n + 2R_c\right) \tag{5}$$

Where Rp, Rn, Rc are the resistances of P, N legs and the conductor, respectively, and they are given as:

$$R_{p,n,c} = L_{p,n,c}\rho_{p,n,c}/A_{p,n,c} \tag{6}$$

A, ρ and L in the above equation are the cross-sectional area, the length, electrical resistivity and the length of P-N legs and conductor (c), respectively.

The total resistance of the thermoelectric generator when load resistance R_T is linked with its boundaries is expressed as:

$$R_T = R_i + R_l \tag{7}$$

the output power the thermoelectric generator can produce is as follows:

$$P = \left((\alpha_p - \alpha_n)(T_h - T_c)/R_t\right)^2 R_l \tag{8}$$

T_h and T_c refer to the temperature of hot and cold ceramic plates of the thermoelectric generator. When the internal resistance is equal in value to the load resistance, maximum output power could be obtained.

2.2 Governing Equations

Based on above-mentioned assumptions, the mass conservation, momentum and energy equations used in the 3D model are written as:

- Mass conservation

$$\frac{\partial u}{\partial x} + \frac{\partial v}{\partial y} + \frac{\partial w}{\partial z} = 0 \tag{9}$$

- Momentum equations

$$\rho_{nf}\left(u\frac{\partial u}{\partial x} + v\frac{\partial u}{\partial y} + w\frac{\partial u}{\partial z}\right) = -\frac{\partial p}{\partial x} + \mu_{nf}\left(\frac{\partial^2 u}{\partial x^2} + \frac{\partial^2 u}{\partial y^2} + \frac{\partial^2 u}{\partial z^2}\right) \tag{10}$$

$$\rho_{nf}\left(u\frac{\partial v}{\partial x} + v\frac{\partial v}{\partial y} + w\frac{\partial v}{\partial z}\right) = -\frac{\partial p}{\partial y} + \mu_{nf}\left(\frac{\partial^2 v}{\partial x^2} + \frac{\partial^2 v}{\partial y^2} + \frac{\partial^2 v}{\partial z^2}\right) \tag{11}$$

$$\rho_{nf}\left(u\frac{\partial w}{\partial x} + v\frac{\partial w}{\partial y} + w\frac{\partial w}{\partial z}\right) = -\frac{\partial p}{\partial z} + \mu_{nf}\left(\frac{\partial^2 w}{\partial x^2} + \frac{\partial^2 w}{\partial y^2}\frac{\partial^2 w}{\partial z^2}\right) \tag{12}$$

- Energy equation

$$\frac{\partial T}{\partial t} + u\frac{\partial T}{\partial x} + v\frac{\partial T}{\partial y} + w\frac{\partial T}{\partial z} = \alpha_{nf}\left(\frac{\partial^2 T}{\partial x^2} + \frac{\partial^2 T}{\partial y^2} + \frac{\partial^2 T}{\partial z^2}\right) \tag{13}$$

Where u, v and w are the components of velocity in the axis (x) ,(y) and (z), respectively. ρ_{nf}, p, and μ_{nf} are density, pressure and dynamic viscosity of water-based SWCNT nanofluid, respectively. Here,

T denotes for temperature, and $\alpha_{nf} = \left(k_{nf}/\rho_{nf}Cp_{nf}\right)$ is the thermal diffusivity, where $k_{nf}$and Cp_{nf} express thermal conductivity and specific heat at constant pressure of employed fluid.

- Equations for the solid domain energy

$$\nabla(k\nabla T) + (J^2/\sigma) - TJ.\nabla s = 0 \tag{14}$$

The continuity equation of electric charge and the coupled equations of heat flux with thermoelectric effect are given as follows:

$$\nabla.J = 0 \tag{15}$$

$$E = \rho J + s\nabla T \tag{16}$$

$$q = \Pi J - k\nabla T \tag{17}$$

Here, Π, J, q, E and are referred to Peltier coefficient, current density, heat flux and electric field respectively.

$$\Pi = sT \tag{18}$$

$$J = \sigma(E - s\nabla T) \tag{19}$$

Where, σ expresses resistivity electric and s denotes the Seebeck coefficient. The relationship between the electric tension V and electric field *E* is given as:

$$E = -\nabla V \tag{20}$$

2.3 Thermo-Physical Properties of Nanofluid

In this model, water-based SWCNT nanofluid was used as a heat transfer improvement technique in order to improve heat exchange between fluid and TEG surfaces. Table 2 shows the thermos-physical properties of constituents of working fluid.

Table 2. Properties of Nanofluids

Properties	Water	SWCNT
ρ (kg/m^3)	997.1	2600
c_p(J/kg k)	4179	425
k (W/m k)	0.61	3000
μ(kg/m s)	8.55x10^5	-

The properties of water-based nanofluid such as density (ρ_{nf}), thermal conductivity (k), dynamic viscosity (μ_{nf}) , heat capacity ($\left(\rho c_p\right)_{nf}$) are computed using the following correlations:

$$\rho_{nf} = (1-\emptyset)\rho_f + \emptyset\rho_p \tag{21}$$

$$\left(\rho c_p\right)_{nf} = (1-\emptyset)\left(\rho c_p\right)_f + \emptyset\left(\rho c_p\right)_p \tag{22}$$

$$\mu_{nf} = u_f/(1-\emptyset)^{2.5} \tag{23}$$

$$k = \left((1-\emptyset) + 2\emptyset(k_{cnt}/k_{cnt} - k_f)\ln(k_{cnt} + k_f/2k_f)\right) \tag{24}$$

In the above equations, the symbol (∅) refers to the volume fraction of nanoparticles and subscript *nf*, *f*, and *p* stand for, nanofluid, base fluid (water) and nanoparticle, respectively.

2.4 Boundary Conditions

Fig. (2) illustrates all boundary conditions of the model. The velocity of nanofluid of both channels (u_h, u_c) is a function of Reynolds number which varies from 50 to 1000. The temperature of the nanofluid entering the hot channel is T_H = 333.15 k, and for the cold channel, T_C = 293.15 k. In this study, all walls are adiabatically isolated and the velocity at walls is considered nil. Lastly, the pressure leaving both channels is considered nul.

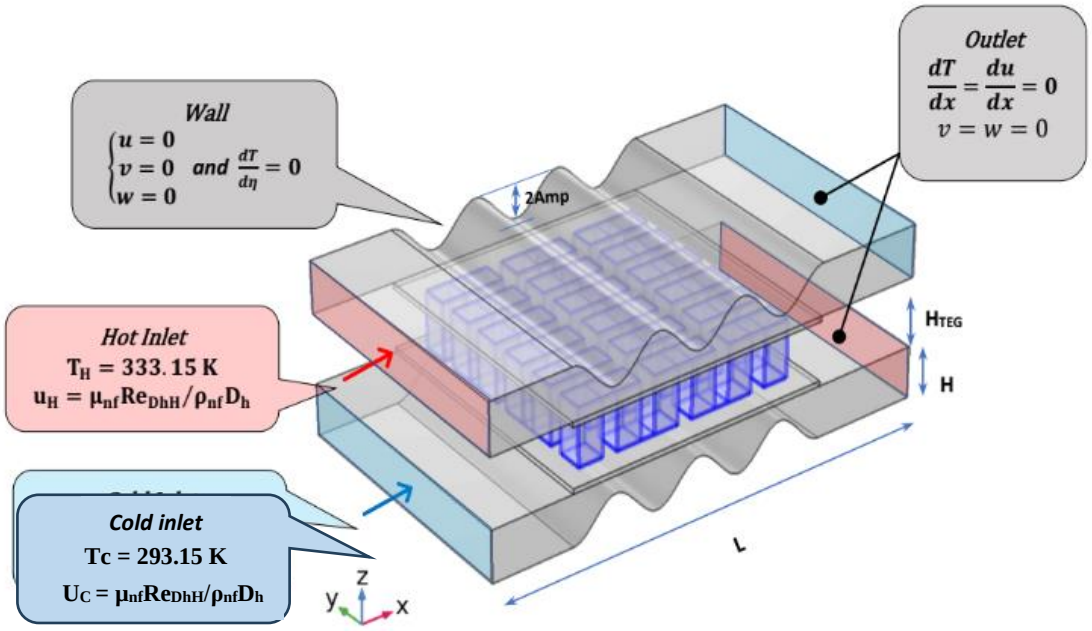

Fig 2. Boundary conditions of the TEG mounted channel

2.5 Numerical Solver

The model under study involves solving fluid flow, heat transfer and electric field physics coupled simultaneously. Therefore, as recommended and used in previous studies for solving Multiphysics phenomena, the finite element method was selected as a numerical method to compute the governing

equations with their boundary conditions, using the generalized minimum residual (GMRES) iterative method to provide accurate results.

2.6 Code Validation and Grid Independence Test

To obtain precise results with independence of mesh element number, a grid test was carried out at different element numbers, attempting to determine an optimum mesh element size with taking into consideration the computation time. Table 3 shows the results of output(P) power, heat absorbed (Q_c) and pressure coefficient (P_c) at different mesh elements. It was apparent from the table that, at grid 7 (G7), with 1386209 mesh elements, the results are very slightly affected by mesh elements, with a relative error of less than 0.03%. For this reason, grid 7 was chosen to perform all simulations of the model.

Table 3. Grid test of thermoelectric generator mounted channel

Grid	Mesh element	P (W)	Q_c	P_c
G1	23822	0.021334	2.2358	9.9253
G2	35940	0.021243	2.0885	10.028
G3	64474	0.021173	2.0942	10.174
G4	115556	0.021020	2.2044	10.150
G5	207217	0.020973	2.2939	9.9881
G6	434533	0.020892	2.4021	9.8929
G7	1386209	0.020815	2.5464	9.8521
G8	4890735	0,020809	2,5471	9,8493

The current model is validated with an experimental study of flow through a wavy channel conducted by (Oviedo-Tolentino et al., 2008), and the comparison is provided in Fig. (3), where it can be seen that the two results agree well. another validation is conducted with the work of (Kramer et al., 2019), when they performed an analytical and numerical investigation of commercial TEHP1263-1.5 thermoelectric generator, aiming to determine the internal resistance, power, current and voltage of TEG. The analogy is drawn in Fig. (4) for the output voltage and isotherm of the thermoelectric generator, and it shows a perfect match.

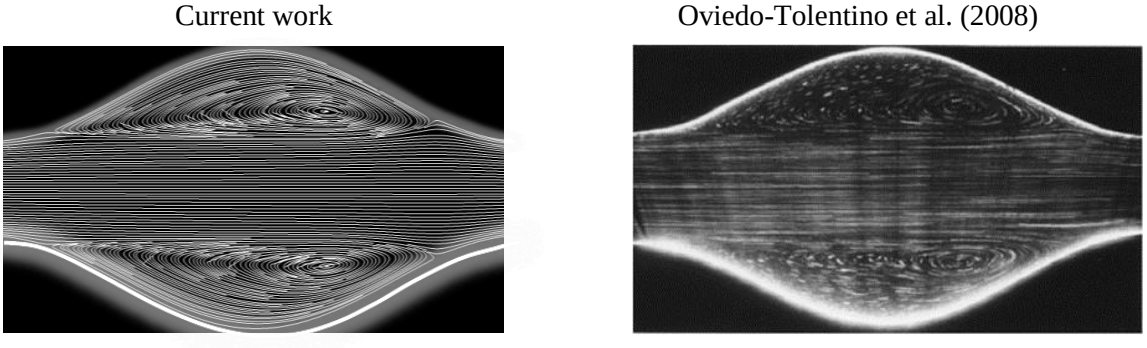

Fig 3. Validation of streamlines with the work of Oviedo-Tolentino et al. (2008)

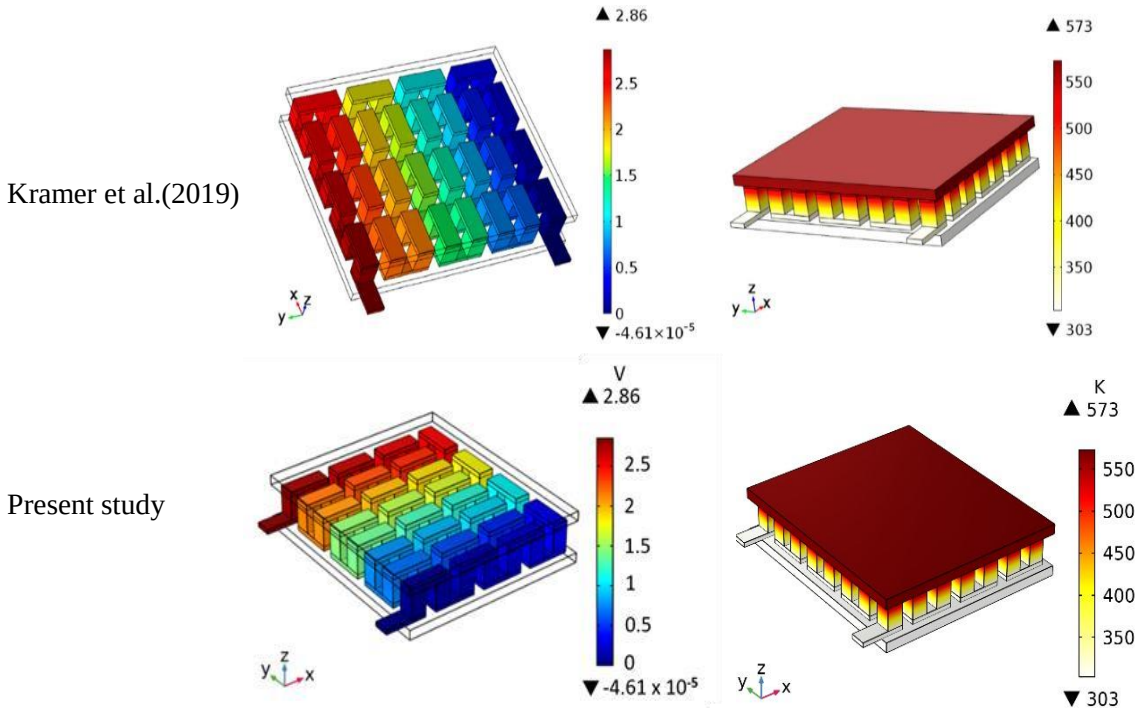

Fig 4. Validation of output voltage and isotherm with the study of Kramer et al. (2019)

3. RESULTS AND DISCUSSION

The present work aims to enhance thermoelectric generator performance by improving heat transfer between nanofluid and thermoelectric generator surfaces. The nanoparticle volume fraction (Φ=0.3%) was set to be constant in all the simulations. The number of waves and Reynolds number were varied from 1 to 5 and from 50 to 1000, respectively.

This section provides simulation results of the influence of channel shape on the electrical energy generation of TEG regarding different Reynold number values.

3.1 Impact of Number of Waves on Power Generation

To understand the influence of the number of waves on the variation of heat transfer rate and thermoelectric performance, streamlines plots of different numbers of waves, taken from the longitudinal mid-section of the physical system, are presented in Fig. (5). The value of Reynolds number is 200, and the amplitude of the wave is set to be 1mm. According to this Figure, it is noticeable that there is a change in flow behavior when the shape of the channel is waved, and that is accompanied by formation of recirculation zones just after throttling of flow, which provokes acceleration of flow, and the magnitude of those vortices increases with the increase of wave number. It was observed that the higher the number of waves, the more velocity of flow is generated.

Fig. (6) shows the influence of the number of waves on the streamlines and isotherm of TEG mounted channel. It is apparent from the graph the insignificance of increasing the number of waves on the temperature change and velocity of the nanofluid. That is, no change in the maximal velocity of channels when the number of waves n varies from 1 to 5. For isotherm, just less than one degree Celsius of temperature is incremented when moving from 1 wave to 5 ones. Figure (7) gives a detailed description of the influence of the number of waves on the average temperature of ceramic plates of TEG.

.

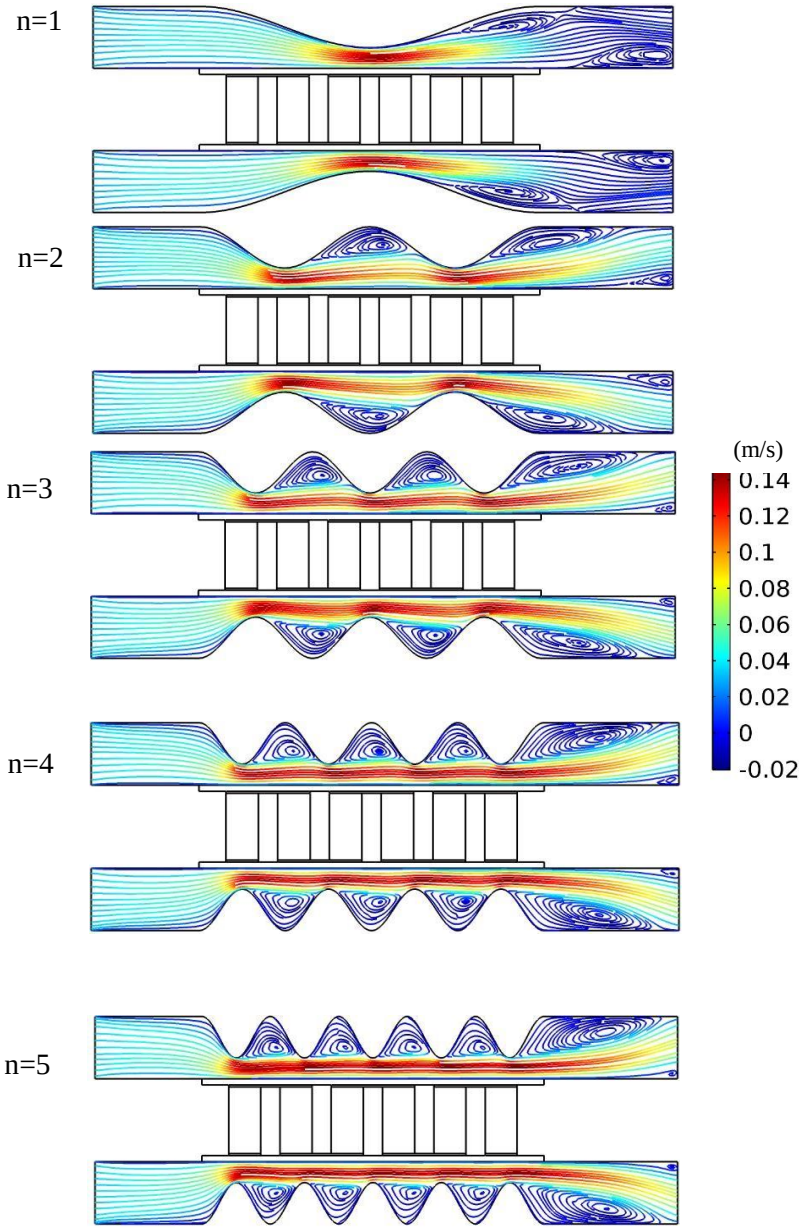

Fig 5. Streamlines of TEG with different number of waves

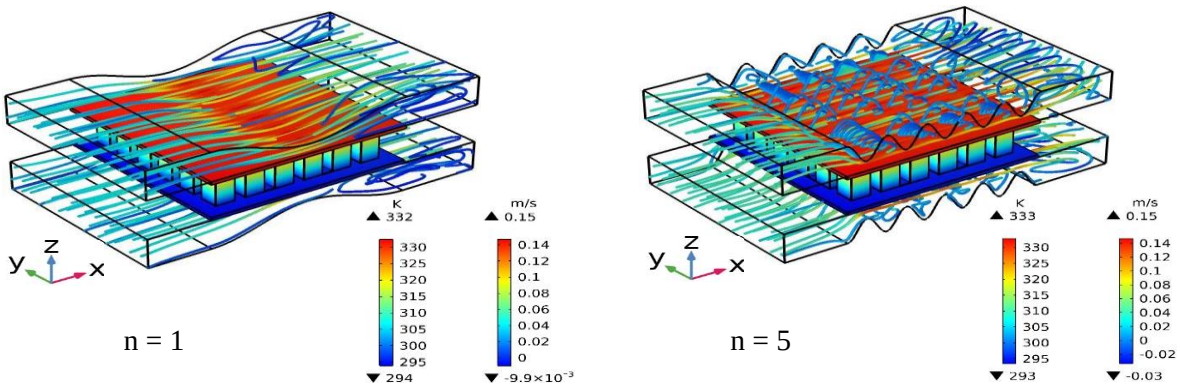

Fig 6. 3D Streamlines and isotherm of TEG mounted channels with different number of waves

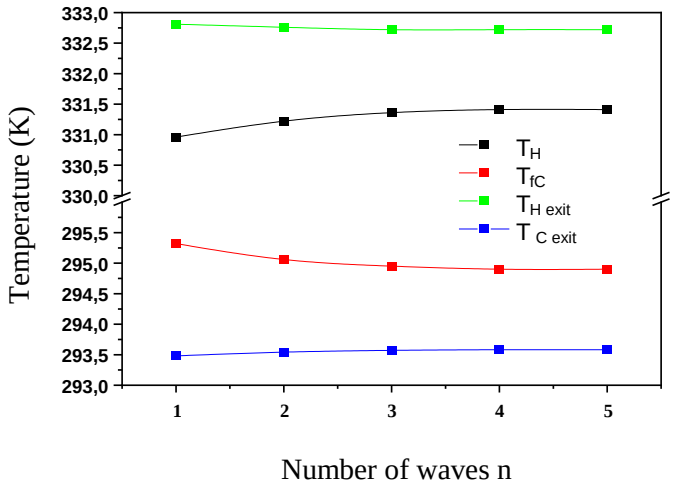

Fig 7. Impact of number of waves on average temperature of TEG ceramic plates

To see the impact of wave number on the generated power of TEG, Fig. (8) is plotted, notably, the variation of power is very low, from 0.014 w to 0.022 w when the number of waves changes from 1 to 5, similarly for produced voltage of TEG as depicted in Fig. (9). When n is more than 3, the generated power tends to be constant. Therefore, the influence of wave number on the output power of TEG is very subtle and limited, and this is due to little heat change between ceramic plates and nanofluid.

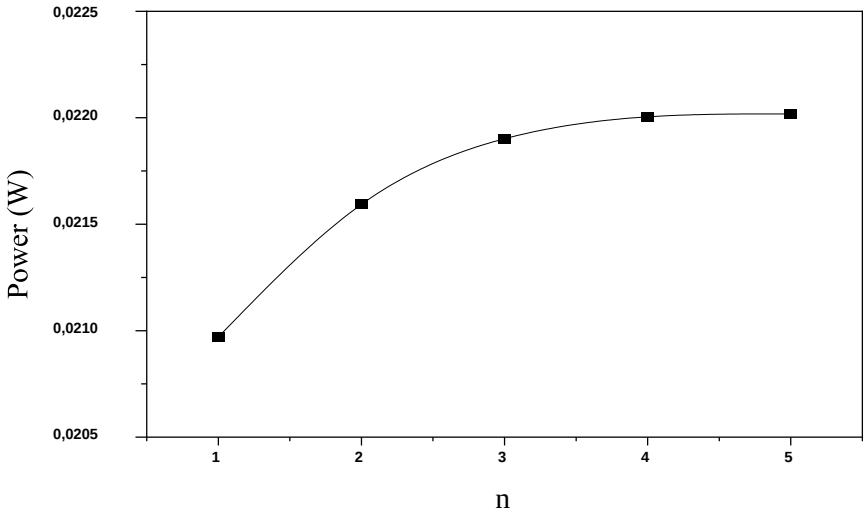

Fig 8. Influence of number of waves n on generated power of TEG

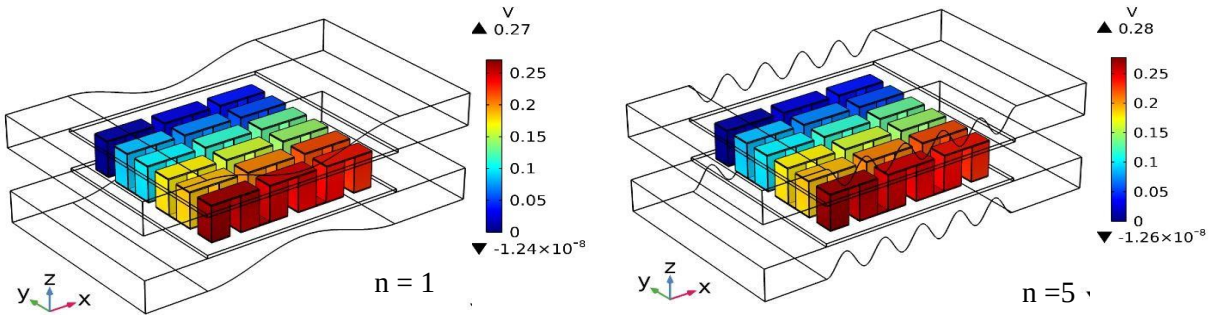

Fig 9. Produced voltage of TEG at n=1, n=5

3.2 Influence of Reynolds Number on TEG Power Generation

In order to clarify how Reynolds number affects TEG power augmentation, Fig. (10) is plotted. The figure shows the streamlines contour of fluid flow in the upper and lower channels at different Reynolds numbers (50, 100, 200, 600, 1000). A closer examination of this figure reveals that increasing Reynolds number causes a remarkable change in fluid flow and a substantial increase in vortices magnitude, formed after the throttling regions in the channels. At a low value of Re (50), vortices begin to appear at a very small scale. When Re becomes greater, the separation of flow occurs, and the intensity of vortices becomes larger; as well as the velocity gradient significantly changes as the Reynolds number rises. Fig. (11) presents the relationship between generated power and Reynolds number. As the Re is incremented, which means that the velocity of the fluid is increased, TEG produces more electric power, and that can result in diminishing thermal boundary layer thickness between nanofluid and ceramic plates, as Fig. (12) illustrates the average temperature of upper and lower ceramic plates of TEG.

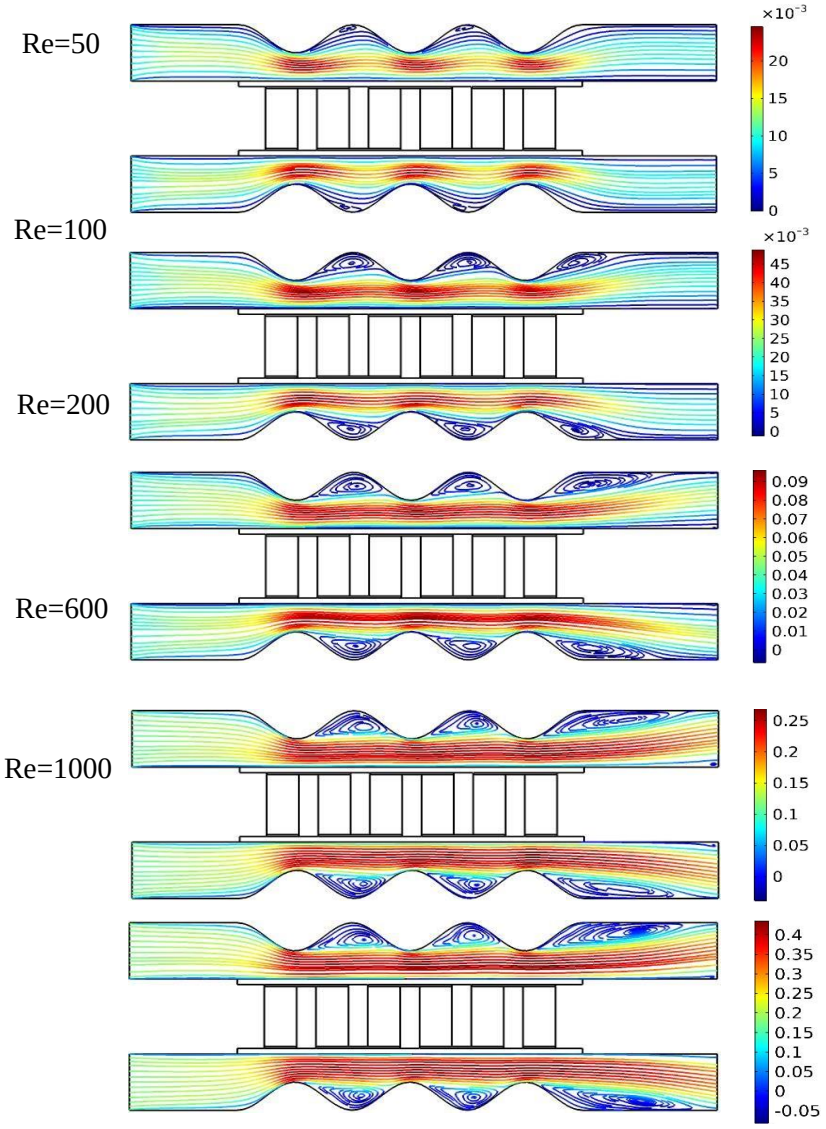

Fig 10. Streamlines of TEG at different Reynolds numbers

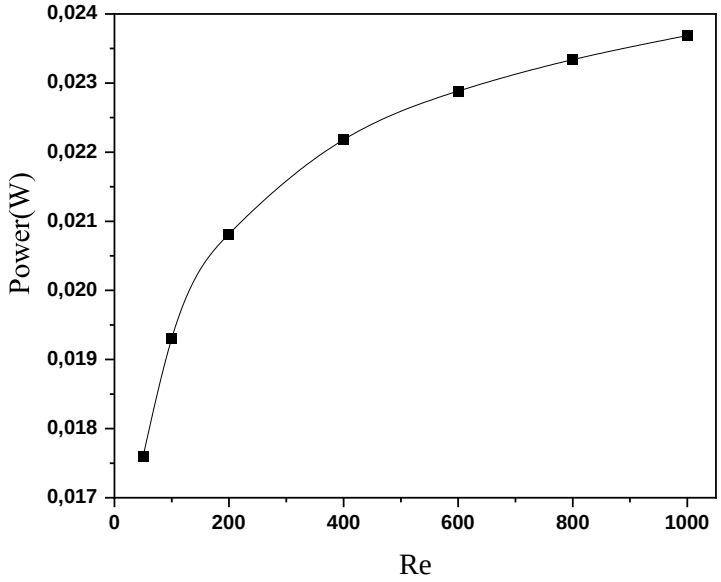

Fig 11. Relationship between power of TEG and Reynolds number

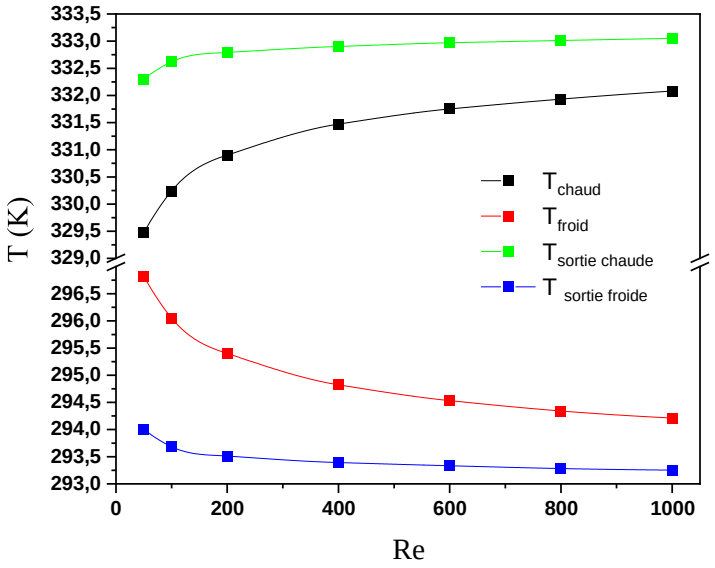

Fig 12. Average temperature of ceramic plates at various Reynolds numbers

4. CONCLUSION

In this work, the power generation of thermoelectric generator mounted wavy channel flowing nanofluid is numerically studied. The nanofluid contains water-based single-walled carbon nanotubes with a 0.3% volume fraction. The influence of the number of waves, from 1 to 5, and the Reynolds number (between 50 and 1000) were deeply investigated. The output voltage, power of TEG, and the distribution of temperature of ceramic plates are computed. The following outcomes are obtained:

- The corrugated wall channel increases the heat transfer rate, and therefore the thermal and electric performance of the thermoelectric generator are improved.
- Reynolds number plays a significant role in enhancing the power generation of TEG, increasing it leads to a remarkable increase of generated power of TEG.
- The increment of the number of waves has a limited impact on enhancing power generation of TEG, an increase of 0.1% of power is observed when varying the number of waves from 1 to 5.

REFERENCES

Aridi, R., Faraj, J., Ali, S., Lemenand, T., & Khaled, M. (2021). Thermoelectric Power Generators: State-of-the-Art, Heat Recovery Method, and Challenges. *Electricity*, *2*(3), 359-386. https://www.mdpi.com/2673-4826/2/3/22

Casi, Á., Araiz, M., Catalán, L., & Astrain, D. (2021). Thermoelectric heat recovery in a real industry: From laboratory optimization to reality. *Applied Thermal Engineering*, *184*, 116275. https://doi.org/10.1016/j.applthermaleng.2020.116275

Chen, W.-H., Chiou, Y.-B., Chein, R.-Y., Uan, J.-Y., & Wang, X.-D. (2022). Power generation of thermoelectric generator with plate fins for recovering low-temperature waste heat. *Applied Energy*, *306*, 118012. https://doi.org/10.1016/j.apenergy.2021.118012

Kim, C. S., Lee, G. S., Choi, H., Kim, Y. J., Yang, H. M., Lim, S. H., Lee, S.-G., & Cho, B. J. (2018). Structural design of a flexible thermoelectric power generator for wearable applications. *Applied Energy*, *214*, 131-138. https://doi.org/10.1016/j.apenergy.2018.01.074

Kramer, L. R., Maran, A. L. O., de Souza, S. S., & Ando Junior, O. H. (2019). Analytical and Numerical Study for the Determination of a Thermoelectric Generator's Internal Resistance. *Energies*, *12*(16), 3053. https://www.mdpi.com/1996-1073/12/16/3053

LaLonde, A. D., Pei, Y., Wang, H., & Jeffrey Snyder, G. (2011). Lead telluride alloy thermoelectrics. *Materials Today*, *14*(11), 526-532. https://doi.org/10.1016/S1369-7021(11)70278-4

Luo, D., Yan, Y., Wang, R., & Zhou, W. (2021). Numerical investigation on the dynamic response characteristics of a thermoelectric generator module under transient temperature excitations. *Renewable energy*, *170*, 811-823. https://doi.org/10.1016/j.renene.2021.02.026

Mostafavi, S. A., & Mahmoudi, M. (2018). Modeling and fabricating a prototype of a thermoelectric generator system of heat energy recovery from hot exhaust gases and evaluating the effects of important system parameters. *Applied Thermal Engineering*, *132*, 624-636. https://doi.org/10.1016/j.applthermaleng.2018.01.018

Nugraha, N. A., Baskoro, D. C., Riyadi, T. W. B., & Wijayanta, A. T. (2024). Thermal characteristics of thermoelectric generator at various heating rates: Experimental and numerical assessments. *Thermal Science and Engineering Progress*, *52*, 102671. https://doi.org/10.1016/j.tsep.2024.102671

Orr, B., Akbarzadeh, A., & Lappas, P. (2017). An exhaust heat recovery system utilising thermoelectric generators and heat pipes. *Applied Thermal Engineering*, *126*, 1185-1190. https://doi.org/10.1016/j.applthermaleng.2016.11.019

Oviedo-Tolentino, F., Romero-Méndez, R., Hernández-Guerrero, A., & Girón-Palomares, B. (2008). Experimental study of fluid flow in the entrance of a sinusoidal channel. *International Journal of Heat and Fluid Flow*, *29*(5), 1233-1239. https://doi.org/10.1016/j.ijheatfluidflow.2008.03.017

Polozine, A., Sirotinskaya, S., & Schaeffer, L. (2014). History of Development of Thermoelectric Materials for Electric Power Generation and Criteria of their Quality. *Materials Research-ibero-american Journal of Materials*, *17*, 1260-1267.

Proto, A., Peter, L., Cerny, M., Penhaker, M., Bibbo, D., Conforto, S., & Schmid, M. (2018, 17-20 Sept. 2018). Human Body Energy Harvesting Solutions for Wearable Technologies. 2018 IEEE 20th International Conference on e-Health Networking, Applications and Services (Healthcom),

Scherrer, H., Rowe, D., Kajikawa, T., Matsubara, K., Issi, J.-P., Goldsmid, H. J., Bhandari, C. M., Burkov, A. T., Zaitsev, V. K., & Fedorov, M. I. (2018). Thermoelectrics Handbook: Macro to Nano.

Selimefendigil, F., Omri, M., Aich, W., Besbes, H., Ben Khedher, N., Alshammari, B. M., & Kolsi, L. (2023). Numerical Study of Thermo-Electric Conversion for TEG Mounted Wavy Walled Triangular Vented Cavity Considering Nanofluid with Different-Shaped Nanoparticles. *Mathematics*, *11*(2), 483. https://www.mdpi.com/2227-7390/11/2/483

Selimefendigil, F., & Öztop, H. F. (2023). Impacts of using helical coils (HCs) on the performance improvements of thermoelectric device mounted channels and modeling by using soft computing techniques. *Sustainable Energy Technologies and Assessments*, *56*, 103067. https://doi.org/10.1016/j.seta.2023.103067

Wang, Z., Leonov, V., Fiorini, P., & Van Hoof, C. (2009). Realization of a wearable miniaturized thermoelectric generator for human body applications. *Sensors and Actuators A: Physical*, *156*(1), 95-102. https://doi.org/10.1016/j.sna.2009.02.028

Zhao, Y., Wang, S., Ge, M., Li, Y., & Liang, Z. (2017). Analysis of thermoelectric generation characteristics of flue gas waste heat from natural gas boiler. *Energy Conversion and Management*, *148*, 820-829. https://doi.org/10.1016/j.enconman.2017.06.029

Zoui, M. A., Bentouba, S., Stocholm, J. G., & Bourouis, M. (2020). A Review on Thermoelectric Generators: Progress and Applications. *Energies*, *13*(14), 3606. https://www.mdpi.com/1996-1073/13/14/3606